



Published in final edited form as:

Medchemcomm. 2016 August 1; 7(8): 1672–1680. doi:10.1039/C6MD00277C.

Design, synthesis and evaluation of novel ^{19}F magnetic resonance sensitive protein tyrosine phosphatase inhibitors[†]

Yu Li^a, Guiquan Xia^a, Qi Guo^a, Li Wu^b, Shizhen Chen^c, Zhigang Yang^a, Wei Wang^a, Zhong-Yin Zhang^b, Xin Zhou^c, and Zhong-Xing Jiang^{a,c,d,e}

Zhong-Xing Jiang: zxjiang@whu.edu.cn

^aSchool of Pharmaceutical Sciences, Wuhan University, Wuhan 430071, China

^bDepartment of Medicinal Chemistry and Molecular Pharmacology, Center for Cancer Research, Purdue University, West Lafayette, Indiana 47907, USA

^cState Key Laboratory for Magnetic Resonance and Atomic and Molecular Physics, Wuhan Institute of Physics and Mathematics, Chinese Academy of Sciences, Wuhan 430071, China

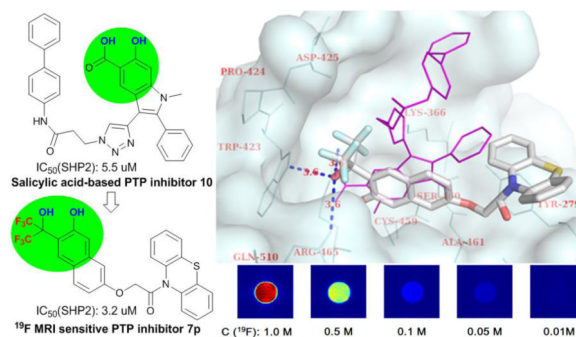
^dKey Laboratory of Synthetic Chemistry of Natural Substances, Shanghai Institute of Organic Chemistry, Chinese Academy of Sciences, Shanghai 200032, China

^eState Key Laboratory for Modification of Chemical Fibers and Polymer Materials, Donghua University, Shanghai 201620, China

Abstract

Fluorine is a highly attractive element for both medicinal chemistry and imaging technologies. To facilitate protein tyrosine phosphatases (PTPs)-targeted drug discovery and imaging-guided PTP research with fluorine, several highly potent and ^{19}F MR sensitive PTP inhibitors were discovered through a structure-based focused library strategy.

Graphical abstract



[†]The authors declare no competing interests.

Correspondence to: Zhong-Xing Jiang, zxjiang@whu.edu.cn.

Electronic Supplementary Information (ESI) available: Copies of ^1H NMR, ^{13}C NMR, ^{19}F NMR and HRMS of compounds, and single-crystal X-ray diffractograms of 7c (CCDC1470244). See DOI: 10.1039/x0xx00000x

The first ^{19}F MRI sensitive PTP inhibitors were discovered through a structure-based focus library strategy. *Ortho*-bis(trifluoromethyl)carbinol phenol not only successfully mimics the interactions between salicylic acid and PTPs, but also sheds new light on PTPs.

Introduction

PTPs play crucial roles in such fundamental cellular processes as proliferation, differentiation, survival, apoptosis, motility and adhesion.¹ Abnormal PTP activity is well known to be associated with a broad spectrum of human diseases.² As a superfamily of more than 100 signalling enzymes, many PTPs have emerged as attractive drug targets, such as mPTPB for tuberculosis, SHP2 for many types of cancers, LYP for autoimmune diseases, PTP1B for type 2 diabetes, obesity and breast cancer.³ To this end, the discovery of highly potent and specific small-molecule PTP inhibitors and their application in probing the biological and pathological mechanisms of PTPs, especially with the aid of modern imaging and spectroscopy technologies, are the cornerstone for PTPs-targeted drug discovery.

As a versatile element in biomedical research, fluorine has promising utility in PTPs-targeted drug discovery. On one hand, the introduction of fluorine(s) into bioactive molecules is usually accompanied by improved pharmacokinetic properties and protein-ligand binding interactions.⁴ Thus, fluorination has become a routine strategy in drug discovery and fluorinated compounds have made up over 20% of all pharmaceuticals. On the other hand, fluorinated molecules can be monitored *in vivo* without ionizing radiation and background signals by ^{19}F magnetic resonance (^{19}F MR) which provides high-contrast and non-invasive spectroscopy (^{19}F NMR) and images (^{19}F MRI). In recent years, ^{19}F MRI/NMR has been widely used in tracking targets of interest⁵ and monitoring biological reactions.⁶ Therefore, the discovery of fluorinated small-molecule PTP inhibitors with high ^{19}F MR sensitivity may provide easy access to PTPs-targeted drugs and detailed understanding of PTPs' biological and pathological mechanisms.

A recent discovery of a ^{19}F MRI sensitive salinomycin derivative with specific toxicity towards cancer cells⁷ by this group promoted us to develop novel fluorinated PTP inhibitors. Herein, *ortho*-bis(trifluoromethyl)carbinol phenol was designed as a novel chemical scaffold for ^{19}F MRI sensitive PTP inhibitors (Scheme 1). Due to the strong electron-withdraw ability of 2 trifluoromethyl groups, the bis(trifluoromethyl)-carbinol is a weak acid and therefore a suitable substitute for the carboxylic group in salicylic acid from which a number of highly potent and selective PTP inhibitors have recently been discovered.⁸ Consequently, the *ortho*-bis(trifluoromethyl)-carbinol phenols may mimic the well-established binding mode of salicylic acid-based inhibitors at the highly positively charged active site of PTPs.⁸ It is noteworthy that the 6 symmetric fluorines in the bis(trifluoromethyl)carbinol, which were recently employed in the construction of highly ^{19}F MRI sensitive dendritic drug delivery vehicles,⁹ aggregately provide a strong ^{19}F MR signal for conveniently probing the mode of interaction and related biological reactions with ^{19}F NMR and ^{19}F MRI. Moreover, cell permeability is a challenge for PTP inhibitors. The bis(trifluoromethyl)carbinol-based PTP inhibitors without negative charge may exhibit favorable cell permeability,

bioavailability and pharmacokinetic properties by the introduction hydrophobic trifluoromethyl groups.⁴

Materials and methods

Chemistry general information

¹H, ¹⁹F and ¹³C NMR spectra were recorded at 400 MHz. Chemical shifts (δ) are in ppm and coupling constants (J) are in Hertz (Hz). ¹H NMR spectra were referenced to tetramethylsilane (d, 0.00 ppm) using CDCl₃, Acetone-d₆ or DMSO-d₆ as solvents. ¹³C NMR spectra were referenced to solvent carbons (77.16 ppm for CDCl₃, 29.84, 206.26 ppm for Acetone-d₆ and 39.52 ppm for DMSO-d₆). ¹⁹F NMR spectra were referenced to 2% perfluorobenzene (s, -164.90 ppm). The splitting patterns for ¹H NMR spectra are denoted as follows: s (singlet), d (doublet), q (quartet), m (multiplet), dd (doublet of doublets), td (triplet of doublets). High resolution mass spectra were recorded using Electron Spray Ionization (ESI).

Unless otherwise indicated, all reagents were obtained from commercial supplier and used without prior purification. DCM and DMF were dried and freshly distilled prior to use. Flash chromatography was performed on silica gel (200–300 mesh) with either petroleum ether/EtOAc as eluents.

Synthesis of Compounds

Phenol 1c—Hexafluoroacetone trihydrate (9.71 g, 6.1 mL, 44.1 mmol) was dried over concentrated sulfuric acid and the resulting anhydrous hexafluoroacetone was bubbled into to a solution of 4-phenylphenol (5.00 g, 29.4 mmol) and aluminium chloride (0.39 g, 2.94 mmol) in 1,2-dichloroethane (250 mL) slowly. After the addition, the mixture was heated to reflux at 80°C until 4-phenylphenol was consumed as indicated by TLC. The reaction mixture was then cooled to rt, washed with 2 N HCl (100 mL) and extracted with DCM (50 mL \times 2). The combined organic layers were dried over anhydrous Na₂SO₄, concentrated under vacuum and purified by flash chromatography on silica gel (5% EtOAc/petroleum ether) to give **1c** as white wax (3.6 g, 85% yield). ¹H NMR (CDCl₃, 400 MHz) δ 7.00 (d, J = 8.5 Hz, 1H), 7.35 (t, J = 7.2 Hz, 1H), 7.44 (t, J = 8.0 Hz, 2H), 7.48–7.54 (m, 2H), 7.57 (dd, J = 8.5, 2.1 Hz, 1H), 7.66 (s, 1H); ¹⁹F NMR (CDCl₃, 376 MHz) δ -78.53; ¹³C NMR (Acetone-d₆, 100 MHz) δ 80.0–81.2 (m), 116.0, 119.5, 124.2 (q, J = 286 Hz), 127.4, 127.7, 128.2, 129.9, 131.0, 134.7, 140.7, 156.6; HRMS (ESI) calcd for C₁₅H₁₁F₆O₂⁺ ([M+H]⁺) 337.0658, found 337.0671.

Phenol 1a—was prepared from benzene by following the general procedure as clear oil (2.5 g, 30%). ¹H NMR (CDCl₃, 400 MHz) δ 7.39–7.53 (m, 3H), 7.73 (dd, J = 7.4, 0.9 Hz, 2H); ¹⁹F NMR (CDCl₃, 376 MHz) δ -78.69.

Phenol 1b—was prepared from *p*-cresol (3.0 g, 27.7 mmol) by following the general procedure as white wax (6.1 g, 80%). ¹H NMR (CDCl₃, 400 MHz) δ 2.31 (s, 3H), 6.16 (s, 1H), 6.81 (d, J = 8.3 Hz, 1H), 6.88 (s, 1H), 7.15 (dd, J = 8.3, 1.6 Hz, 1H), 7.23 (s, 1H); ¹⁹F NMR (CDCl₃, 376 MHz) δ -78.64.

Phenol 1d—Prepared from [1,1'-biphenyl]-3-ol (5.00 g, 29.4 mmol) in the same manner as described for **1c** (8.6 g, 87% yield). ^1H NMR (CDCl_3 , 400 MHz) δ 7.13 (d, J = 1.8 Hz, 1H), 7.19–7.26 (m, 1H), 7.35–7.47 (m, 3H), 7.47–7.59 (m, 3H); ^{19}F NMR (CDCl_3 , 376 MHz) δ –78.72; ^{13}C NMR (Acetone- d_6 , 100 MHz) δ 79.9–81.1 (m), 114.5, 117.0, 120.2, 124.2 (q, J = 286 Hz), 128.8, 129.1, 129.9, 140.0, 145.3, 157.5; HRMS (ESI) calcd for $\text{C}_{15}\text{H}_{11}\text{F}_6\text{O}_2^+$ ($[\text{M}+\text{H}]^+$) 337.0658, found 337.0651.

Phenol 1e—Prepared from [1,1'-biphenyl]-2-ol (5.00 g, 29.4 mmol) in the same manner as described for **1c** (3.6 g, 74% yield). ^1H NMR (CDCl_3 , 400 MHz) δ 7.11 (t, J = 7.9 Hz, 1H), 7.35 (dd, J = 7.5, 1.5 Hz, 1H), 7.43–7.50 (m, 3H), 7.50–7.59 (m, 3H); ^{19}F NMR (CDCl_3 , 376 MHz) δ –78.41; ^{13}C NMR (Acetone- d_6 , 100 MHz) δ 80.6–81.8 (m), 115.5, 121.4, 124.1 (q, J = 286 Hz), 128.2, 128.3, 129.2, 130.5, 133.1, 133.8, 138.4, 154.9; HRMS (ESI) calcd for $\text{C}_{15}\text{H}_{11}\text{F}_6\text{O}_2^+$ ($[\text{M}+\text{H}]^+$) 337.0658, found 337.0654.

Phenol 1f—Prepared from 2-naphthalenol (5.00 g, 34.7 mmol) in the same manner as described for **1c** (6.2 g, 57% yield). ^1H NMR (CDCl_3 , 400 MHz) δ 7.29 (s, 1H), 7.42 (dd, J = 11.1, 3.9 Hz, 1H), 7.52 (dd, J = 11.1, 4.0 Hz, 1H), 7.68 (d, J = 8.3 Hz, 1H), 7.82 (d, J = 8.2 Hz, 1H), 8.04 (s, 1H); ^{19}F NMR (CDCl_3 , 376 MHz) δ –78.40; ^{13}C NMR (Acetone- d_6 , 100 MHz) δ 80.2–81.4 (m), 113.3, 117.7, 124.2 (q, J = 286 Hz), 125.5, 126.6, 128.9, 129.0, 129.5, 130.6, 135.7, 154.0; HRMS (ESI) calcd for $\text{C}_{13}\text{H}_9\text{F}_6\text{O}_2^+$ ($[\text{M}+\text{H}]^+$) 311.0501, found 311.0489.

Phenol 1g—Prepared from 1-naphthalenol (5.00 g, 34.7 mmol) in the same manner as described for **1c** (6.5 g, 60% yield). ^1H NMR (CDCl_3 , 400 MHz) δ 7.39 (s, 2H), 7.46–7.63 (m, 2H), 7.71–7.84 (m, 1H), 8.24–8.38 (m, 1H); ^{19}F NMR (CDCl_3 , 376 MHz) δ –78.55; ^{13}C NMR (Acetone- d_6 , 100 MHz) δ 81.2–82.4 (m), 107.0, 120.6, 123.5, 124.18 (q, J = 287 Hz), 124.19, 126.8, 126.9, 128.2, 129.0, 135.9, 155.5; HRMS (ESI) calcd for ($[\text{M}+\text{H}]^+$) $\text{C}_{13}\text{H}_9\text{F}_6\text{O}_2^+$ 311.0501, found 311.0498.

Naphthol 3—Prepared from 2,7-naphthalenediol (30.0 g, 187.2 mmol) in the same manner as described for **1c** (10.2 g, 17% yield). ^1H NMR (Acetone- d_6 , 400 MHz) δ 7.01–7.13 (m, 2H), 7.25 (s, 1H), 7.85 (d, J = 8.0 Hz, 1H), 8.04 (s, 1H); ^{19}F NMR (Acetone- d_6 , 376 MHz) δ –76.10; ^{13}C NMR (Acetone- d_6 , 100 MHz) δ 80.1–81.3 (m), 107.9, 111.7, 114.2, 118.4, 124.1, 124.3 (q, J = 286 Hz), 130.3, 131.5, 137.6, 154.5, 158.2; HRMS (ESI) calcd for $\text{C}_{13}\text{H}_9\text{F}_6\text{O}_3^+$ ($[\text{M}+\text{H}]^+$) 327.0450, found 327.0444.

Naphthol 4—To an ice-cold suspension of diol **3** (2.40 g, 7.36 mmol) in trifluoroacetic acid was added acetone (2.2 mL, 29.5 mmol), then TFA (10.8 mL, 145.87 mmol) was added to the mixture dropwise. The reaction mixture was warmed slowly to rt and then stirred for 48 h. After evaporation of the solvent, the residue was purified by flash chromatography on silica gel (2% EtOAc/petroleum ether) to give **4** as white wax (0.85 g, 34% yield). ^1H NMR (Acetone- d_6 , 400 MHz) δ 1.61 (s, 6H), 7.11–7.24 (m, 2H), 7.34 (s, 1H), 7.95 (d, J = 8.8 Hz, 1H), 8.09 (s, 1H); ^{19}F NMR (Acetone- d_6 , 376 MHz) δ –78.30; ^{13}C NMR (Acetone- d_6 , 100 MHz) δ 27.0, 76.6–77.8 (m), 102.8, 108.5, 110.0, 113.7, 119.2, 123.2 (q, J = 287 Hz),

125.2, 128.4, 131.6, 138.0, 150.0, 158.5; HRMS (ESI) calcd for $C_{16}H_{13}F_6O_3^+$ ($[M+H]^+$) 367.0763, found 367.0773.

Ester 8—To a solution of **4** (470.0 mg, 1.28 mmol) and methyl bromoacetate (588.7 mg, 3.85 mmol) in acetone was added K_2CO_3 (381.5 mg, 3.85 mmol), then the reaction mixture was heated at reflux until **4** was consumed as indicated by TLC. After removal of the solvent under reduced pressure, the residue was dissolved in EtOAc (20 mL), and washed with water (50 mL \times 2). The organic layer was dried over anhydrous Na_2SO_4 , concentrated under vacuum and purified by flash chromatography on silica gel (2% EtOAc/petroleum ether) to give ester **8** as light yellow oil (480.0 mg, 86% yield). 1H NMR ($CDCl_3$, 400 MHz) δ 1.60 (s, 6H), 3.83 (s, 3H), 4.76 (s, 2H), 6.96 (d, $J = 2.4$ Hz, 1H), 7.19 (dd, $J = 9.0, 2.5$ Hz, 1H), 7.29 (s, 1H), 7.78 (d, $J = 9.0$ Hz, 1H), 7.99 (s, 1H); ^{19}F NMR ($CDCl_3$, 376 MHz) δ -78.24; ^{13}C NMR ($CDCl_3$, 100 MHz) δ 26.8, 52.4, 65.2, 76.0–76.6 (m), 101.8, 105.5, 113.6, 118.3, 122.1 (q, $J = 287$ Hz), 125.1, 127.6, 130.7, 136.2, 149.5, 157.5, 169.0; HRMS (ESI) calcd for $C_{19}H_{17}F_6O_5^+$ ($[M+H]^+$) 439.0975, found 439.0981.

Acid 9—Ester **8** (400.0 mg, 0.91 mmol) was dissolved in THF/ H_2O (5 mL/5 mL) and the solution was stirred at 0°C. Then NaOH (43.8 mg, 1.10 mmol, 10 N aqueous solution) was added at 0°C. The reaction mixture was stirred at rt until **8** was consumed as indicated by TLC. The solution was acidified to pH 6.0, then extracted with EtOAc (20 mL \times 2) and washed with water (10 mL). The organic layer was dried over anhydrous Na_2SO_4 and concentrated under vacuum to give acid **9** as white wax (370 mg, 96% yield). 1H NMR ($CDCl_3$, 400 MHz) δ 1.60 (s, 6H), 4.82 (s, 2H), 6.99 (d, $J = 2.4$ Hz, 1H), 7.19 (dd, $J = 9.0, 2.5$ Hz, 1H), 7.29 (s, 1H), 7.79 (d, $J = 9.1$ Hz, 1H), 7.99 (s, 1H); ^{19}F NMR ($CDCl_3$, 376 MHz) δ -78.33; ^{13}C NMR (Acetone- d_6 , 100 MHz) δ 27.0, 65.4, 76.6–77.8 (m), 102.9, 106.6, 111.0, 114.6, 119.5, 123.2 (q, $J = 286$ Hz), 126.0, 128.4, 131.5, 137.6, 150.2, 159.0, 170.0; HRMS (ESI) calcd for $C_{18}H_{15}F_6O_5^+$ ($[M+H]^+$) 425.0818, found 425.0798.

Amide 7a—Potassium carbonate (170.0 mg, 1.23 mmol) was added to a solution of **4** (150.0 mg, 0.41 mmol) and **6a** (111.6 mg, 0.62 mmol) in acetone (5 mL), then the result suspension was heated at reflux until **4** was consumed as indicated by TLC. After removal of the solvent under reduced pressure, the residue was dissolved in EtOAc (25 mL), washed with 2N HCl (30 mL) and brine (30 mL \times 2). The organic layer was dried over anhydrous Na_2SO_4 , concentrated under vacuum and used without purification. The residue was dissolved in TFA/ H_2O (9/1, 11.3 mL), then anisole (45 μ L) was added and the resulting mixture was stirred overnight. The reaction mixture was concentrated under vacuum and then diluted with EtOAc (25 mL), washed with brine (30 mL \times 2), the organic layer was dried over anhydrous Na_2SO_4 , concentrated under vacuum and purified by flash chromatography on silica gel (20–80% EtOAc/petroleum ether) to give **7a** as clear oil (131 mg, 77% yield). 1H NMR (Acetone- d_6 , 400 MHz) δ 0.88 (t, $J = 7.4$ Hz, 3H), 1.41–1.66 (m, 2H), 3.24–3.31 (m, 2H), 4.64 (s, 2H), 7.09–7.25 (m, 2H), 7.42 (s, 1H), 7.91 (d, $J = 9.0$ Hz, 1H), 8.09 (s, 1H); ^{19}F NMR (Acetone- d_6 , 376 MHz) δ -76.08; ^{13}C NMR (Acetone- d_6 , 100 MHz) δ 11.1, 23.0, 41.0, 67.4, 79.7–80.3 (m), 105.4, 111.9, 114.8, 117.8, 123.6 (q, $J = 286$ Hz), 124.1, 129.5, 130.8, 136.6, 154.4, 157.8, 168.6; HRMS (ESI) calcd for $C_{18}H_{18}F_6NO_4^+$ ($[M+H]^+$) 426.1135, found 426.1118.

Amide 7b—Prepared from **4** (110.0 mg, 0.30 mmol) in the same manner as described for **7a** (100 mg, 78% yield). ^1H NMR (Acetone- d_6 , 400 MHz) δ 0.48–0.64 (m, 2H), 0.66–0.80 (m, 2H), 2.06 (dt, J = 4.4, 2.2 Hz, 1H), 4.61 (s, 2H), 7.08–7.23 (m, 2H), 7.42 (s, 1H), 7.90 (d, J = 9.0 Hz, 1H), 8.08 (s, 1H); ^{19}F NMR (Acetone- d_6 , 376 MHz) δ -76.06; ^{13}C NMR (Acetone- d_6 , 100 MHz) δ 5.9, 22.8, 67.6, 79.9–80.5 (m), 105.5, 112.1, 114.9, 117.9, 123.8 (q, J = 286 Hz), 124.2, 129.7, 131.0, 136.7, 154.5, 158.0; HRMS (ESI) calcd for $\text{C}_{18}\text{H}_{16}\text{F}_6\text{NO}_4^+$ ($[\text{M}+\text{H}]^+$) 424.0978, found 424.0976.

Amide 7c—Prepared from **4** (150.0 mg, 0.41 mmol) in the same manner as described for **7a** (130 mg, 72% yield). ^1H NMR (Acetone- d_6 , 400 MHz) δ 1.12 (t, J = 7.1 Hz, 3H), 1.26 (t, J = 8.0 Hz, 3H), 3.42 (q, J = 7.0 Hz, 2H), 3.51 (q, J = 7.1 Hz, 2H), 4.95 (s, 2H), 7.02–7.18 (m, 2H), 7.30 (s, 1H), 7.85 (d, J = 8.8 Hz, 1H), 8.02 (s, 1H); ^{19}F NMR (Acetone- d_6 , 376 MHz) δ -76.04; ^{13}C NMR (Acetone- d_6 , 100 MHz) δ 12.8, 14.1, 40.6, 66.0, 78.0–79.2 (m), 104.7, 110.0, 116.5, 122.4, 123.1 (q, J = 288 Hz), 129.6, 130.2, 136.0, 153.9, 157.6, 166.0; HRMS (ESI) calcd for $\text{C}_{19}\text{H}_{20}\text{F}_6\text{NO}_4^+$ ($[\text{M}+\text{H}]^+$) 440.1291, found 440.1298.

Amide 7d—Prepared from **4** (150.0 mg, 0.41 mmol) in the same manner as described for **7a** (90 mg, 42% yield). ^1H NMR (DMSO- d_6 , 400 MHz) δ 1.62 (s, 6H), 2.00 (d, J = 10.7 Hz, 10H), 4.53 (s, 2H), 7.06 (d, J = 8.4 Hz, 2H), 7.18 (s, 1H), 7.44 (s, 1H), 7.85 (d, J = 8.7 Hz, 1H); ^{19}F NMR (DMSO- d_6 , 376 MHz) δ -76.01; ^{13}C NMR (DMSO- d_6 , 100 MHz) δ 28.7, 35.9, 40.9, 51.0, 67.0, 78.0–79.1 (m), 104.6, 110.1, 116.6, 122.5, 123.1 (q, J = 288 Hz), 129.6, 130.2, 136.0, 153.9, 157.3, 166.4; HRMS (ESI) calcd for $\text{C}_{25}\text{H}_{26}\text{F}_6\text{NO}_4^+$ ($[\text{M}+\text{H}]^+$) 518.1761, found 518.1766.

Amide 7e—Prepared from **4** (100.0 mg, 0.27 mmol) in the same manner as described for **7a** (91 mg, 71% yield). ^1H NMR (Acetone- d_6 , 400 MHz) δ 4.51 (d, J = 8.0 Hz, 2H), 4.71 (s, 2H), 7.10–7.16 (m, 1H), 7.17–7.33 (m, 6H), 7.40 (s, 1H), 7.89 (d, J = 8.0 Hz, 1H), 8.08 (s, 1H); ^{19}F NMR (Acetone- d_6 , 376 MHz) δ -76.03; ^{13}C NMR (DMSO- d_6 , 100 MHz) δ 41.8, 67.0, 78.0–78.9 (m), 104.8, 110.1, 116.7, 122.6, 123.1 (q, J = 287 Hz), 126.7, 127.1, 128.2, 129.7, 130.2, 136.0, 139.3, 153.9, 157.1, 167.6; HRMS (ESI) calcd for $\text{C}_{22}\text{H}_{18}\text{F}_6\text{NO}_4^+$ ($[\text{M}+\text{H}]^+$) 474.1135, found 474.1138.

Amide 7f—Prepared from **4** (150.0 mg, 0.41 mmol) in the same manner as described for **7a** (200 mg, 99% yield). ^1H NMR (Acetone- d_6 , 400 MHz) δ 4.50 (d, J = 5.9 Hz, 2H), 4.72 (d, J = 2.0 Hz, 2H), 6.98–7.07 (m, 2H), 7.13 (dd, J = 9.0, 2.5 Hz, 1H), 7.20 (d, J = 2.4 Hz, 1H), 7.30–7.38 (m, 2H), 7.42 (s, 1H), 7.90 (d, J = 9.0 Hz, 1H), 8.09 (s, 1H); ^{19}F NMR (Acetone- d_6 , 376 MHz) δ -117.73, -76.14; ^{13}C NMR (DMSO- d_6 , 100 MHz) δ 41.1, 67.0, 78.0–79.2 (m), 104.8, 110.2, 114.8, 115.0, 116.7, 122.6, 123.1 (q, J = 287 Hz), 129.0, 129.1, 129.7, 130.2, 135.5, 136.0, 153.9, 157.1, 159.9, 162.3, 167.6; HRMS (ESI) calcd for $\text{C}_{22}\text{H}_{17}\text{F}_7\text{NO}_4^+$ ($[\text{M}+\text{H}]^+$) 492.1040, found 492.1041.

Amide 7g—Prepared from **4** (150.0 mg, 0.41 mmol) in the same manner as described for **7a** (170 mg, 78% yield). ^1H NMR (Acetone- d_6 , 400 MHz) δ 3.65 (s, 3H), 3.74 (s, 3H), 4.43 (d, J = 6.2 Hz, 2H), 4.70 (s, 2H), 6.81 (d, J = 1.0 Hz, 2H), 6.89 (s, 1H), 7.08–7.26 (m, 2H), 7.39 (s, 1H), 7.90 (d, J = 9.0 Hz, 1H), 8.09 (s, 2H); ^{19}F NMR (Acetone- d_6 , 376 MHz) δ

–76.03; ^{13}C NMR (Acetone- d_6 , 100 MHz) δ 42.7, 55.4, 55.6, 67.5, 79.8–80.4 (m), 105.6, 112.0, 112.1, 115.0, 118.0, 120.2, 123.8 (q, J = 286 Hz), 124.2, 129.7, 131.0, 131.8, 136.7, 149.1, 149.8, 154.4, 158.0, 168.8; HRMS (ESI) calcd for $\text{C}_{24}\text{H}_{22}\text{F}_6\text{NO}_6^+$ ($[\text{M}+\text{H}]^+$) 534.1346, found 534.1369.

Amide 7h—Prepared from **4** (150.0 mg, 0.41 mmol) in the same manner as described for **7a** (210 mg, 95% yield). ^1H NMR (Acetone- d_6 , 400 MHz) δ 2.98 (t, J = 7.0 Hz, 2H), 3.59 (dd, J = 13.2, 6.8 Hz, 2H), 4.65 (s, 2H), 7.03–7.21 (m, 3H), 7.26 (d, J = 8.2 Hz, 1H), 7.35–7.47 (m, 2H), 7.91 (d, J = 9.0 Hz, 2H); ^{19}F NMR (Acetone- d_6 , 376 MHz) δ –75.99; ^{13}C NMR (Acetone- d_6 , 100 MHz) δ 33.2, 39.0, 67.7, 80.0–80.6 (m), 105.7, 112.2, 115.1, 118.2, 123.9 (q, J = 287 Hz), 124.5, 127.7, 129.4, 129.9, 131.2, 132.9, 133.0, 135.2, 136.4, 137.9, 154.5, 158.1, 168.9; HRMS (ESI) calcd for $\text{C}_{23}\text{H}_{18}\text{Cl}_2\text{F}_6\text{NO}_4^+$ ($[\text{M}+\text{H}]^+$) 556.0512, found 556.0510.

Amide 7i—Prepared from **4** (115.1 mg, 0.31 mmol) in the same manner as described for **7a** (28 mg, 16% yield). ^1H NMR (Acetone- d_6 , 400 MHz) δ 4.84 (s, 2H), 6.26 (s, 1H), 7.05 (dd, J = 9.0, 2.5 Hz, 1H), 7.21–7.32 (m, 3H), 7.36–7.43 (m, 3H), 7.51 (d, J = 7.5 Hz, 2H), 7.81 (t, J = 8.4 Hz, 3H), 8.04 (s, 1H); ^{19}F NMR (Acetone- d_6 , 376 MHz) δ –76.08; ^{13}C NMR (DMSO- d_6 , 100 MHz) δ 54.3, 67.3, 78.8–79.4 (m), 105.1, 110.6, 117.1, 120.6, 123.0, 123.7 (q, J = 288 Hz), 125.2, 128.0, 128.9, 130.1, 130.7, 136.5, 140.6, 144.9, 154.9, 157.7, 169.0; HRMS (ESI) calcd for $\text{C}_{28}\text{H}_{20}\text{F}_6\text{NO}_4^+$ ($[\text{M}+\text{H}]^+$) 548.1291, found 548.1284.

Amide 7j—Prepared from **4** (150.0 mg, 0.41 mmol) in the same manner as described for **7a** (88 mg, 95% yield). ^1H NMR (Acetone- d_6 , 400 MHz) δ 4.81 (s, 2H), 7.11 (t, J = 7.4 Hz, 1H), 7.20–7.39 (m, 4H), 7.42 (s, 1H), 7.72–7.83 (m, 2H), 7.95 (d, J = 9.0 Hz, 1H), 8.12 (s, 1H); ^{19}F NMR (Acetone- d_6 , 376 MHz) δ –76.04; ^{13}C NMR (Acetone- d_6 , 100 MHz) δ 67.7, 79.7–80.3 (m), 105.6, 111.9, 114.8, 117.9, 120.5, 123.6 (q, J = 286 Hz), 124.2, 124.5, 129.0, 129.6, 130.9, 136.6, 138.6, 154.2, 157.9, 166.8; HRMS (ESI) calcd for $\text{C}_{21}\text{H}_{16}\text{F}_6\text{NO}_4^+$ ($[\text{M}+\text{H}]^+$) 460.0978, found 460.0982.

Amide 7k—Prepared from **4** (150.0 mg, 0.41 mmol) in the same manner as described for **7a** (130 mg, 63% yield). ^1H NMR (Acetone- d_6 , 400 MHz) δ 1.20 (d, J = 6.9 Hz, 6H), 2.71–2.98 (m, 1H), 4.81 (s, 2H), 7.12–7.33 (m, 4H), 7.42 (s, 1H), 7.60–7.73 (m, 2H), 7.93 (d, J = 9.0 Hz, 1H), 8.12 (s, 1H); ^{19}F NMR (Acetone- d_6 , 376 MHz) δ –76.11; ^{13}C NMR (Acetone- d_6 , 100 MHz) δ 23.9, 33.8, 67.9, 79.8–80.4 (m), 105.7, 112.1, 114.9, 118.0, 120.8, 123.7 (q, J = 287 Hz), 124.3, 127.0, 129.7, 131.0, 136.3, 136.7, 145.2, 154.3, 158.0, 166.7; HRMS (ESI) calcd for $\text{C}_{24}\text{H}_{22}\text{F}_6\text{NO}_4^+$ ($[\text{M}+\text{H}]^+$) 502.1448, found 502.1424.

Amide 7l—Prepared from **4** (120.0 mg, 0.33 mmol) in the same manner as described for **7a** (47 mg, 27% yield). ^1H NMR (Acetone- d_6 , 400 MHz) δ 4.82 (s, 2H), 7.18–7.29 (m, 2H), 7.34 (d, J = 7.4 Hz, 1H), 7.44 (dd, J = 16.7, 8.8 Hz, 3H), 7.60–7.70 (m, 4H), 7.83–7.98 (m, 3H), 8.09 (s, 1H); ^{19}F NMR (Acetone- d_6 , 376 MHz) δ –76.04; ^{13}C NMR (Acetone- d_6 , 100 MHz) δ 68.0, 80.0–80.5 (m), 105.9, 112.2, 115.0, 118.2, 120.9, 121.0, 123.9 (q, J = 286 Hz), 124.4, 127.1, 127.6, 127.7, 127.8, 129.4, 130.0, 131.1, 136.8, 137.2, 138.3, 140.9, 154.4, 158.1, 167.0; HRMS (ESI) calcd for $\text{C}_{27}\text{H}_{20}\text{F}_6\text{NO}_4^+$ ($[\text{M}+\text{H}]^+$) 536.1291, found 536.1272.

Amide 7m—1,3-diisopropylcarbodiimide (42.8 mg, 0.34 mmol) was added slowly to a solution of acid **9** (120.0 mg, 0.28 mmol) and 1-hydroxytriazole (45.8 mg, 0.34 mmol) in dry DMF (3 mL) at 0°C. After 15 minutes, a solution of 4-morpholinoaniline (60.5 mg, 0.34 mmol) in dry DMF (2 mL) was added and the resulting mixture was stirred at rt overnight. The reaction mixture was diluted with brine (40 mL) and extracted with EtOAc (20 mL × 2). The organic layer was dried over anhydrous Na₂SO₄, concentrated under vacuum and used without purification. The residue was dissolved in TFA/H₂O (v/v, 9/1, 7.6 mL), then anisole (30 μl) was added and the resulting mixture was stirred overnight. The reaction mixture was concentrated under vacuum and then diluted with EtOAc (20 mL), washed with brine (30 mL × 2), the organic layer was dried over anhydrous Na₂SO₄, concentrated under vacuum and purified by flash chromatography on silica gel (20–80% EtOAc/petroleum ether) to give **7m** as white wax (115 mg, 75% yield). ¹H NMR (Acetone-d₆, 400 MHz) δ 3.03–3.17 (m, 4H), 3.71–3.83 (m, 4H), 4.77 (s, 2H), 6.93 (d, *J* = 9.0 Hz, 2H), 7.17–7.31 (m, 2H), 7.42 (s, 1H), 7.57–7.69 (m, 2H), 7.94 (d, *J* = 8.9 Hz, 1H), 8.10 (s, 1H); ¹⁹F NMR (Acetone-d₆, 376 MHz) δ -76.06; ¹³C NMR (DMSO-d₆, 100 MHz) δ 48.8, 66.0, 67.2, 78.3–78.9 (m), 104.7, 110.2, 115.3, 116.6, 121.0, 122.6, 123.1 (q, *J* = 286 Hz), 129.7, 130.3, 136.0, 147.6, 153.9, 157.3, 165.7; HRMS (ESI) calcd for C₂₅H₂₃F₆N₂O₅⁺ ([M+H]⁺) 545.1506, found 545.1490.

Amide 7n—Prepared from **4** (150.0 mg, 0.41 mmol) in the same manner as described for **7a** (120 mg, 57% yield). ¹H NMR (Acetone-d₆, 400 MHz) δ 4.98 (s, 2H), 7.29–7.41 (m, 2H), 7.41–7.60 (m, 4H), 7.76–8.06 (m, 5H), 8.14 (s, 1H); ¹⁹F NMR (Acetone-d₆, 376 MHz) δ -76.07; ¹³C NMR (Acetone-d₆, 100 MHz) δ 68.1, 80.0–80.6 (m), 105.8, 112.1, 115.0, 118.3, 122.6, 122.8, 124.5, 123.9 (q, *J* = 287 Hz), 126.0, 126.6, 126.7, 126.8, 128.87, 128.90, 129.8, 131.2, 133.1, 134.8, 136.8, 154.4, 158.1, 167.8; HRMS (ESI) calcd for C₂₅H₁₈F₆NO₄⁺ ([M+H]⁺) 510.1135, found 510.1110.

Amide 7o—Prepared from **4** (110.0 mg, 0.30 mmol) in the same manner as described for **7a** (110 mg, 68% yield). ¹H NMR (Acetone-d₆, 400 MHz) δ 4.79 (s, 2H), 6.98–7.11 (m, 2H), 7.39 (d, *J* = 45.1 Hz, 1H), 7.81–7.95 (m, 1H), 8.06 (s, 1H); ¹⁹F NMR (Acetone-d₆, 376 MHz) δ -76.07; ¹³C NMR (DMSO-d₆, 100 MHz) δ 66.03, 78.4–80.0 (m), 104.5, 110.2, 116.2, 122.5, 123.2 (q, *J* = 288 Hz), 129.6, 130.3, 136.0, 154.3, 157.3, 166.7; HRMS (ESI) calcd for C₂₇H₂₀F₆NO₄⁺ ([M+H]⁺) 536.1291, found 536.1296.

Amide 7p—Prepared from **4** (150.0 mg, 0.41 mmol) in the same manner as described for **7a** (53 mg, 35% yield). ¹H NMR (Acetone-d₆, 400 MHz) δ 5.06 (s, 2H), 6.86–7.02 (m, 2H), 7.26–7.49 (m, 4H), 7.52–7.65 (m, 2H), 7.65–7.89 (m, 4H), 8.03 (s, 1H); ¹⁹F NMR (Acetone-d₆, 376 MHz) δ -76.12; ¹³C NMR (DMSO-d₆, 100 MHz) δ 65.5, 78.0–79.2 (m), 104.0, 104.1, 110.0, 116.4, 122.5, 123.1 (q, *J* = 286 Hz), 126.9, 127.5, 128.1, 129.6, 130.3, 132.0, 135.76, 135.83, 136.8, 137.2, 137.5, 153.88, 153.93, 156.0, 157.0, 166.0; HRMS (ESI) calcd for C₂₇H₂₀F₆NO₄⁺ ([M+H]⁺) 536.1291, found 536.1296.

Amide 7q—Prepared from **9** (200.0 mg, 0.47 mmol) in the same manner as described for **7m** (126 mg, 76% yield). ¹H NMR (Acetone-d₆, 400 MHz) δ 5.09 (s, 2H), 7.24–7.54 (m, 5H), 7.77 (d, *J* = 8.0 Hz, 1H), 7.96 (dd, *J* = 12.5, 5.3 Hz, 2H), 8.11 (s, 1H); ¹⁹F NMR (Acetone-d₆, 376 MHz) δ -76.12; ¹³C NMR (Acetone-d₆, 100 MHz) δ 67.5, 80.0–81.1 (m),

106.0, 112.4, 115.3, 118.3, 121.8, 122.2, 124.1 (q, $J = 286$ Hz), 124.70, 124.74, 127.0, 130.1, 131.4, 133.0, 137.0, 149.6, 154.8, 158.1, 158.3, 168.2; HRMS (ESI) calcd for $C_{22}H_{15}F_6N_2O_4S^+$ ($[M+H]^+$) 517.0651, found 517.0646.

Amide 7r—Prepared from **9** (120.0 mg, 0.28 mmol) in the same manner as described for **7m** (95 mg, 61% yield). 1H NMR (Acetone- d_6 , 400 MHz) δ 2.34 (s, 3H), 4.65 (s, 2H), 7.03–7.16 (m, 2H), 7.21 (d, $J = 8.1$ Hz, 2H), 7.37 (s, 1H), 7.67 (d, $J = 8.3$ Hz, 2H), 7.89 (dd, $J = 22.1, 8.7$ Hz, 1H), 8.12 (s, 1H); ^{19}F NMR (Acetone- d_6 , 376 MHz) δ -76.03; ^{13}C NMR (Acetone- d_6 , 100 MHz) δ 21.1, 66.7, 79.9–80.5 (m), 105.7, 112.1, 118.2, 123.8 (q, $J = 286$ Hz), 124.4, 128.8, 130.0, 131.1, 136.1, 136.8, 144.5, 154.4, 158.0, 167.1; HRMS (ESI) calcd for $C_{22}H_{19}F_6N_2O_6S^+$ ($[M+H]^+$) 553.0863, found 553.0861.

^{19}F MRI experiments

^{19}F MRI experiments were performed on a 9.4 T microimaging system with a 10 mm inner diameter ^{19}F coil (376.4 MHz) for both radiofrequency transmission and reception. The MSME (Multi Slice Multi Echo) pulse sequence was employed for all MRI acquisitions with single average. FOV = 8×8 mm², SI = 40.0 mm TR = 2500 ms and TE = 7.6 ms were used. The data collection time was 160 ms.

Computational analysis

For computational analysis, PDB code 3O5X was used as model structure. Molecular docking was done using AutoDock Vina. Small molecule binding mode was modelled manually using Moloc (Gerber Molecular Design: Switzerland). The image was produced by PyMOL.

PTPs activity assay

PTP activity was assayed using *p*-nitrophenyl phosphate (pNPP) as a substrate in 3,3-dimethylglutarate buffer (50 mM 3,3-dimethylglutarate, pH 7.0, 1 mM EDTA, 150 mM NaCl) at 25 °C. The library compounds were screened in a 96-well format. The amount of product *p*-nitrophenol was determined from the absorbance at 405 nm detected by a Spectra MAX340 microplate spectrophotometer (Molecular Devices). The nonenzymatic hydrolysis of pNPP was corrected by measuring the control without the addition of enzyme. All PTPs used in the study were recombinant proteins prepared in-house.

Results and discussion

To probe the structure-activity relationship of the *ortho*-bis(trifluoromethyl)carbinol phenol-based inhibitors, a structure-based focused library strategy was employed. Our initial effort involved the construction of a focused library of 7 bis(trifluoromethyl)carbinol-substituted benzene to identify the optimal relative positions for these substituents (Scheme 2). Through the Lewis acid-catalysed Friedel-Crafts reaction, the bis(trifluoromethyl)-carbinol moiety was conveniently anchored to benzene, phenols, and naphthols with good yields. Due to the strong directing effect of phenolic hydroxyl group, the desired *ortho*-bis(trifluoromethyl)carbinol phenols were isolated as the major products (**1b–g**).

The ability of library compounds **1a–g** to inhibit a selected panel of PTPs of therapeutic interest, including mPTPB, SHP2, PTP1B, CD45, LYP, and FAP-1, was assessed at pH 7 and 25°C (Table 1). The results indicate that the phenolic hydroxyl group plays a crucial role in PTP binding through which the inhibitors may mimic the binding mode of salicylic acid-based inhibitors. No appreciable activity was found for **1a**, which lacks phenolic hydroxyl group in the scaffold. The PTP inhibitory activity is also very sensitive to the size and position of substituent. Neither **1c** with a *para*-phenyl group nor **1d** with a *meta*-phenyl group has appreciable activity, while **1b** with a small-sized *para*-methyl group has moderate activity. Among the library compounds **1a–g**, 2-naphthol derived **1f** is the most potent one for the selected panel of PTPs which was then selected for further optimization.

To further improve the potency and selectivity, **1f** was modified into a focused library to target both the active site and a peripheral secondary binding site of PTPs (Scheme 3).^{8,10} Starting from 2,7-naphthalene-diol **2**, a core compound **3**, with an extra 7-hydroxyl group compared to **1f**, was constructed through Friedel-Crafts reaction with good yield. Then, a panel of amines **5a–r** with structural diversity were selected for the side chains **6a–r** construction by reacting with bromoacetyl bromide, respectively. After protecting the 2 neighbouring hydroxyl groups in **3** with acetones, side chains **6a–r** were anchored to the 7-hydroxyl group in **4** in the presence of K₂CO₃ to give ester intermediates after which the acetonide protecting group was removed with TFA to give amides **7a–p** with good yields over 2 steps. However, the preparation of **7m**, **7q** and **7r** was unsuccessful. So, an alternative method was developed by first anchoring an acetic acid side chain to **4** and then coupling amines **5m**, **5q**, and **5r**, respectively, to give the corresponding amides **7m**, **7q**, and **7r**. In these ways, the focused library of 18 *ortho*-bis(trifluoromethyl)carbinol phenols **7a–r** with an amide side chain was conveniently prepared.

To illustrate the structures of *ortho*-bis(trifluoro methyl)carbinol phenols **7a–r**, a single-crystal X-ray structure of **7c** was obtained (Fig. 1). However, many attempts to prepare a single-crystal of **7p** were unsuccessful.

As expected, the activities of library compounds **7a–r** are much higher than these of **1f** (Table 2). Compound **7r** with sulfonhyrazide side chain was identified as a highly potent and selective mPTPB inhibitor with an IC₅₀ value of 2.3 μM and more than 7-fold selectivity compared to SHP2, PTP1B, CD45, LYP, and FAP-1. It is interesting to point out that most of aliphatic amine derived compounds **7a–c** and **7e–g** show no appreciable PTP inhibitory activity, while bulky aliphatic amine derived compounds **7d**, **7h**, and **7i** exhibit moderate activities. In contrast, most of aromatic amine derived compounds **7j–r** have good activities and selectivity except for the positively charged **7m**. Among them, compound **7p** with a bulky aromatic group on the side chain exhibits very high activity toward the selected panel of PTPs with IC₅₀ ranging from 2.2 μM for FAP-1 to 6.6 μM for PTP1B. Based on these observation, it is obvious that the potency of *ortho*-bis(trifluoromethyl) carbinol phenols-based inhibitors can be considerably optimized up to 58-fold by tethering an amide side chain. A bulky aromatic group containing side chain, i.e. **7l** and **7p**, can efficiently promote the binding affinity between PTPs and inhibitors by interacting with a peripheral pocket in the vicinity of the PTPs active sites, probably through steric effects and π-π stacking.

Computational analysis of the binding activity of **7p** in the highly conservative active site of PTPs provided some insight into the structure-activity relationship between these novel inhibitors and PTPs. Oncogenic SHP2 with known complex structure (PDB ID: 3O5X) was selected as a model. Fig. 2 shows the binding mode of **7p** with SHP2 compared to that of a known salicylic acid-based SHP2 inhibitor **10** which has a IC_{50} of 5.5 μ M toward SHP2.^{8a} As expected, *ortho*-bis(trifluoromethyl) carbinol phenol moiety can mimic the binding mode of salicylic acid by interacting with the corresponding amino acid residues Trp423, Arg465 and Gln510 (the distances between O of *ortho*-bis(trifluoromethyl)carbinol and the three hydrogen bonding heavy atoms of the residues are 3.6 Å). However, due to the difference in molecular geometry, the side chains of **7p** and **10** interacted with SHP2 in different ways. Instead of interacting with Arg362 and Lys364 of SHP2, the aromatic side chain in **7p** has a strong π - π interaction with Tyr-279.

Finally, ¹⁹F magnetic resonance properties of PTP inhibitors **7a-r** were investigated. As designed, all 6 symmetrical fluorines in **7a-r** generated a strong singlet ¹⁹F NMR signal, respectively (Fig. 3). Uniformed ¹⁹F signal dramatically improved the ¹⁹F NMR sensitivity of these fluorinated inhibitors for downstream applications. Then, **7p** with high potencies toward a panel of PTPs was selected for ¹⁹F MRI study. It was found that **7p** has a very short longitudinal relaxation time T_1 of 299 ms which could further improve its ¹⁹F MRI sensitivity by allowing the collection of more transient signals without prolonging the data acquisition time. ¹⁹F MRI phantom experiment on an array of **7p** solution indicated that **7p** could be clearly imaged by ¹⁹F MRI with a scan time of 120 seconds at a concentration of as low as 8.3 mM (or 50 mM in ¹⁹F concentration, Fig. 3). Therefore, **7p** is a novel PTP inhibitor as well as a highly valuable tool molecule whose local information, such as distribution and concentration, and interactions with PTPs, such as binding mode and affinity, can be conveniently monitored by ¹⁹F MR spectroscopy and imaging without extra modification in the absence of background signals.

Conclusions and outlook

In summary, we have successfully demonstrated a strategy of developing novel ¹⁹F magnetic resonance sensitive small molecule PTP inhibitors for drug discovery and biomedical research through rational molecular design and symmetrical fluorination. *Ortho*-bis(trifluoromethyl)carbinol phenol is a valuable substitute for salicylic acid in PTP inhibitor discovery, which successfully integrates the PTP binding ability and high ¹⁹F NMR signal generating ability. As fluorinated drugs are booming in pharmaceutical industry, it is of great importance to utilize their inherent ¹⁹F magnetic resonance properties in target identification, pharmacology study, *in vivo* drug tracking, image/spectroscopy-guided drug therapy and beyond.

Finally, we want to point out that both ¹⁹F NMR and ¹⁹F MRI are valuable modalities for biomedical research. ¹⁹F MRI provides high-contrast images at ¹⁹F concentrations of mM and above, while ¹⁹F NMR provides sensitive spectroscopies even at sub- μ M ¹⁹F concentrations. Improving the PTP inhibition potency and selectivity, ¹⁹F MRI sensitivity of these inhibitors and their application in ¹⁹F magnetic resonance-guided PTP mechanism study are currently in progress and will be published in due course.

Supplementary Material

Refer to Web version on PubMed Central for supplementary material.

Acknowledgments

We are thankful for financial support from the National Natural Science Foundation of China (21372181, 21402144, 21572168, and 21575157), Key Laboratory of Synthetic Chemistry of Natural Substances (Shanghai Institute of Organic Chemistry) and State Key Laboratory for Modification of Chemical Fibers and Polymer Materials (Donghua University). LW and ZYZ are supported by NIH RO1 CA69202 and P30 CA023168.

Notes and references

1. Tonks NK. *Nat. Rev. Mol. Cell Biol.* 2006; 7:833. [PubMed: 17057753]
2. (a) Zhang Z-Y. *Curr. Opin. Chem. Biol.* 2001; 5:416. [PubMed: 11470605] (b) Bialy L, Waldmann H. *Angew. Chem., Int. Ed.* 2005; 44:3814.
3. (a) Krause DS, van Etten RA. *New Engl. J. Med.* 2005; 353:172. [PubMed: 16014887] (b) Jiang Z-X, Zhang Z-Y. *Cancer metastasis Rev.* 2008; 27:263. [PubMed: 18259840]
4. Muller K, Faeh C, Diederich F. *Science.* 2007; 317:1881. [PubMed: 17901324]
5. (a) Ahrens ET, Flores R, Xu H, Morel PA. *Nat. Biotechnol.* 2005; 23:983. [PubMed: 16041364] (b) Vivian D, Cheng K, Khurana S, Xu S, Kriel EH, Dawson PA, Raufman JP, Polli JE. *Mol. Pharmaceutics.* 2014; 11:1575.
6. (a) Mizukami S, Takikawa R, Sugihara F, Hori Y, Tochio H, Walchli M, Shirakawa M, Kikuchi K. *J. Am. Chem. Soc.* 2008; 130:794. [PubMed: 18154336] (b) Bruemmer KJ, Merrikhihaghi S, Lollar CT, Morris SN, Bauer JH, Lippert AR. *Chem. Commun.* 2014; 50:12311.
7. Shi Q, Li Y, Bo S, Li X, Zhao P, Liu Q, Yang Z, Cong H, Deng H, Chen M, Chen S, Zhou X, Ding H, Jiang Z-X. *Chem. Commun.* 2016; 52:5136–5139.
8. (a) Zhang X, He Y, Liu S, Yu Z, Jiang Z-X, Yang Z, Dong Y, Nabinger SC, Wu L, Gunawan AM, Wang L, Chan RJ, Zhang Z-Y. *J. Med. Chem.* 2010; 53:2482. [PubMed: 20170098] (b) He Y, Xu J, Yu Z-H, Gunawan AM, Wu L, Wang L, Zhang Z-Y. *J. Med. Chem.* 2013; 56:832. [PubMed: 23305444] (c) He Y, Liu S, Menon A, Stanford S, Oppong E, Gunawan AM, Wu L, Wu DJ, Barrios AM, Bottini N, Cato AC, Zhang Z-Y. *J. Med. Chem.* 2013; 56:4990. [PubMed: 23713581] (d) Zeng LF, Zhang R-Y, Yu Z-H, Liu S, Wu L, Gunawan AM, Lane BS, Mali RS, Li X, Chan RJ, Kapur R, Wells CD, Zhang Z-Y. *J. Med. Chem.* 2014; 57:6594. [PubMed: 25003231]
9. (a) Yu W, Yang Y, Bo S, Li Y, Chen S, Yang Z, Zheng X, Jiang Z-X, Zhou X. *J. Org. Chem.* 2015; 80:4443. [PubMed: 25849491] (b) Bo S, Song C, Li Y, Yu W, Chen S, Zhou X, Yang Z, Zheng X, Jiang Z-X. *J. Org. Chem.* 2015; 80:6360. [PubMed: 26016450]
10. (a) Puius YA, Zhao Y, Sullivan M, Lawrence DS, Almo SC, Zhang Z-Y. *Proc. Natl. Acad. Sci., USA.* 1997; 94:13420. [PubMed: 9391040] (b) Yu X, Sun J-P, He Y, Guo X-L, Liu S, Zhou B, Hudmon A, Zhang Z-Y. *Proc. Natl. Acad. Sci., USA.* 2007; 104:19767. [PubMed: 18056643]

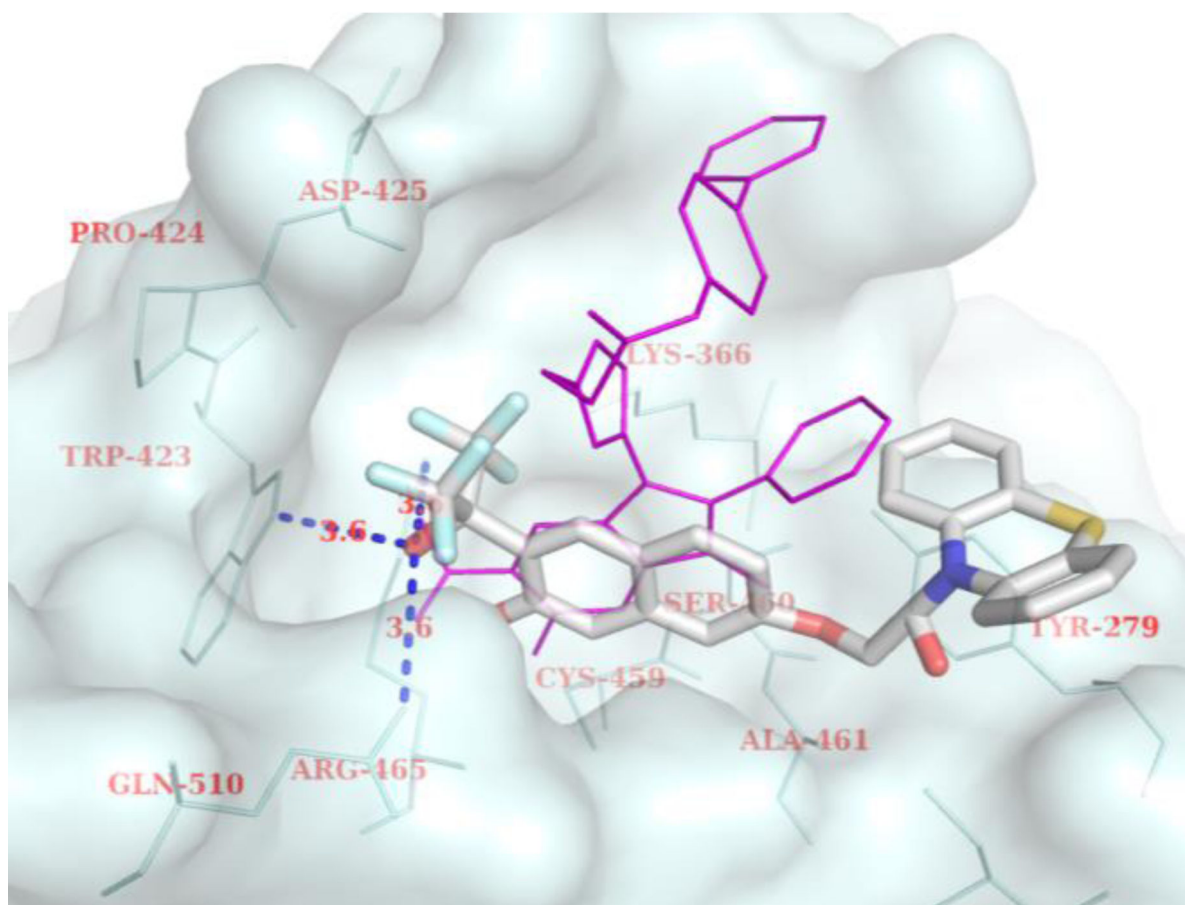
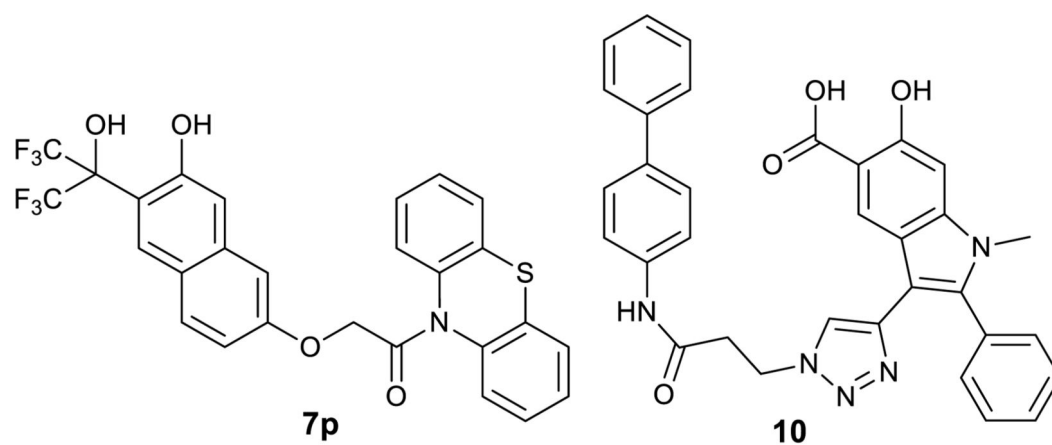


Fig. 2. Calculated structure of **7p** bound to SHP2 with salicylic acid-based inhibitor **10** as a comparison.

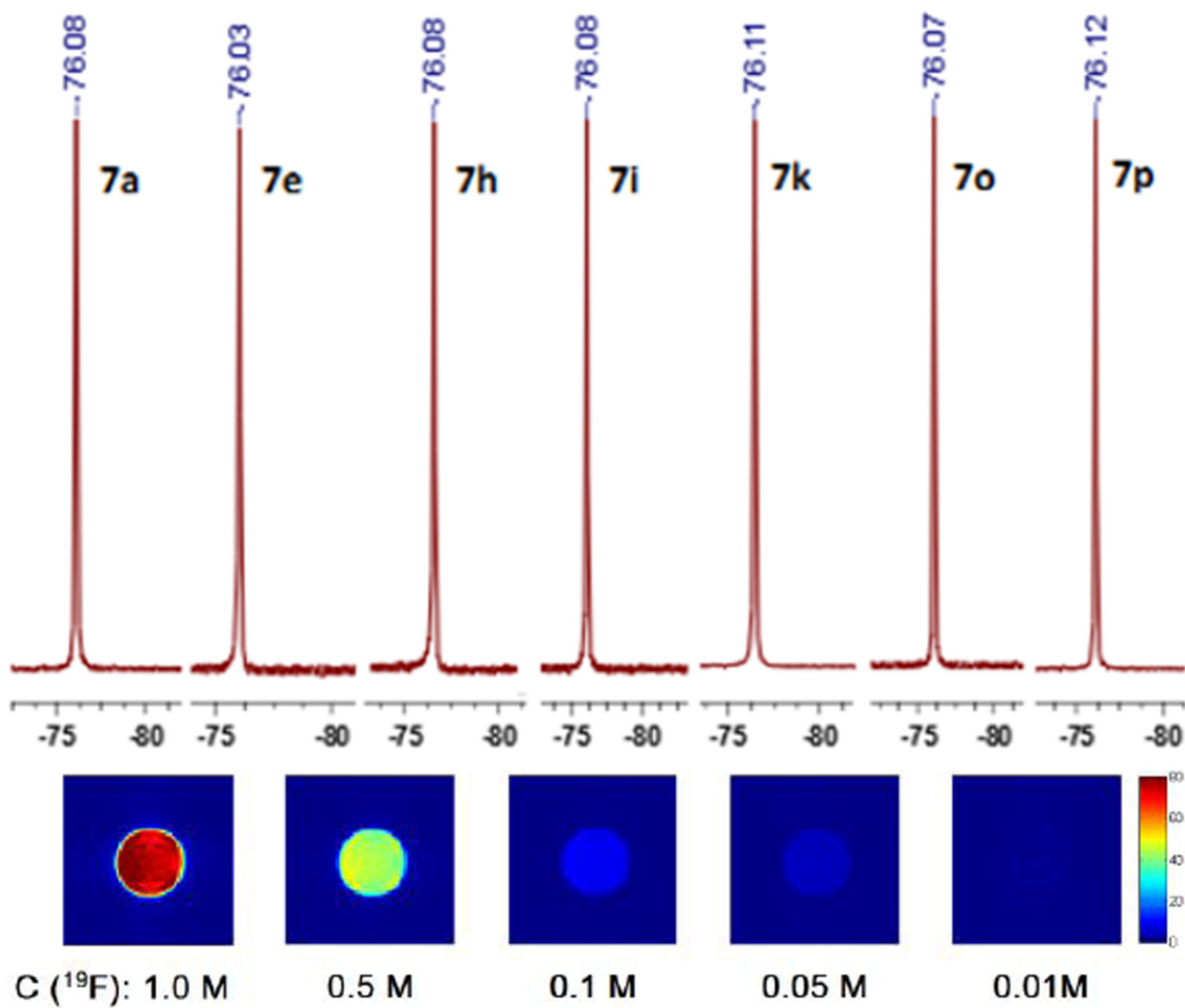
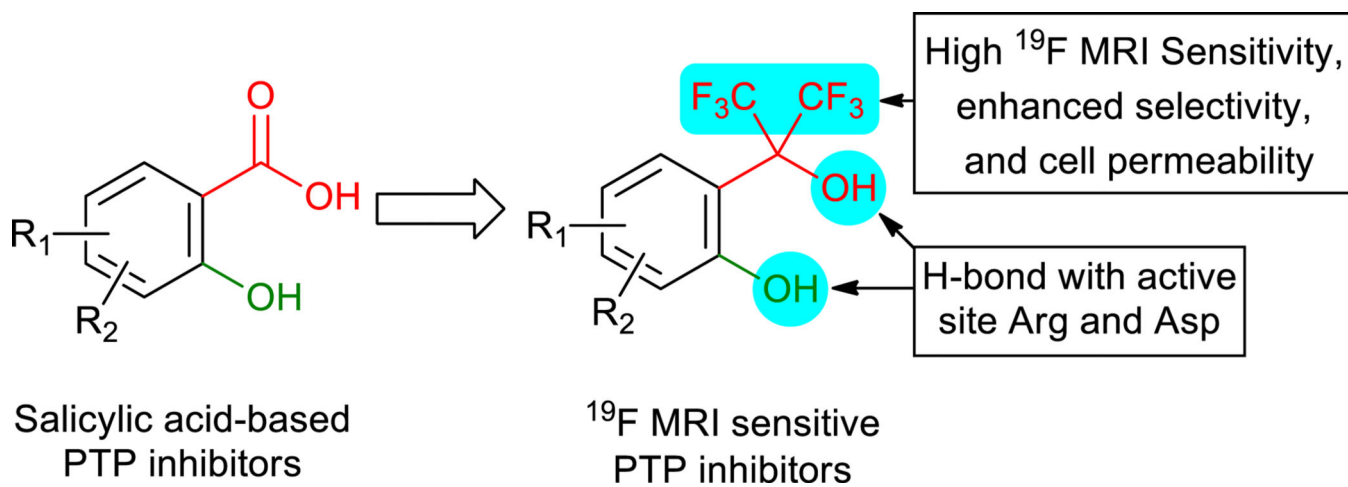
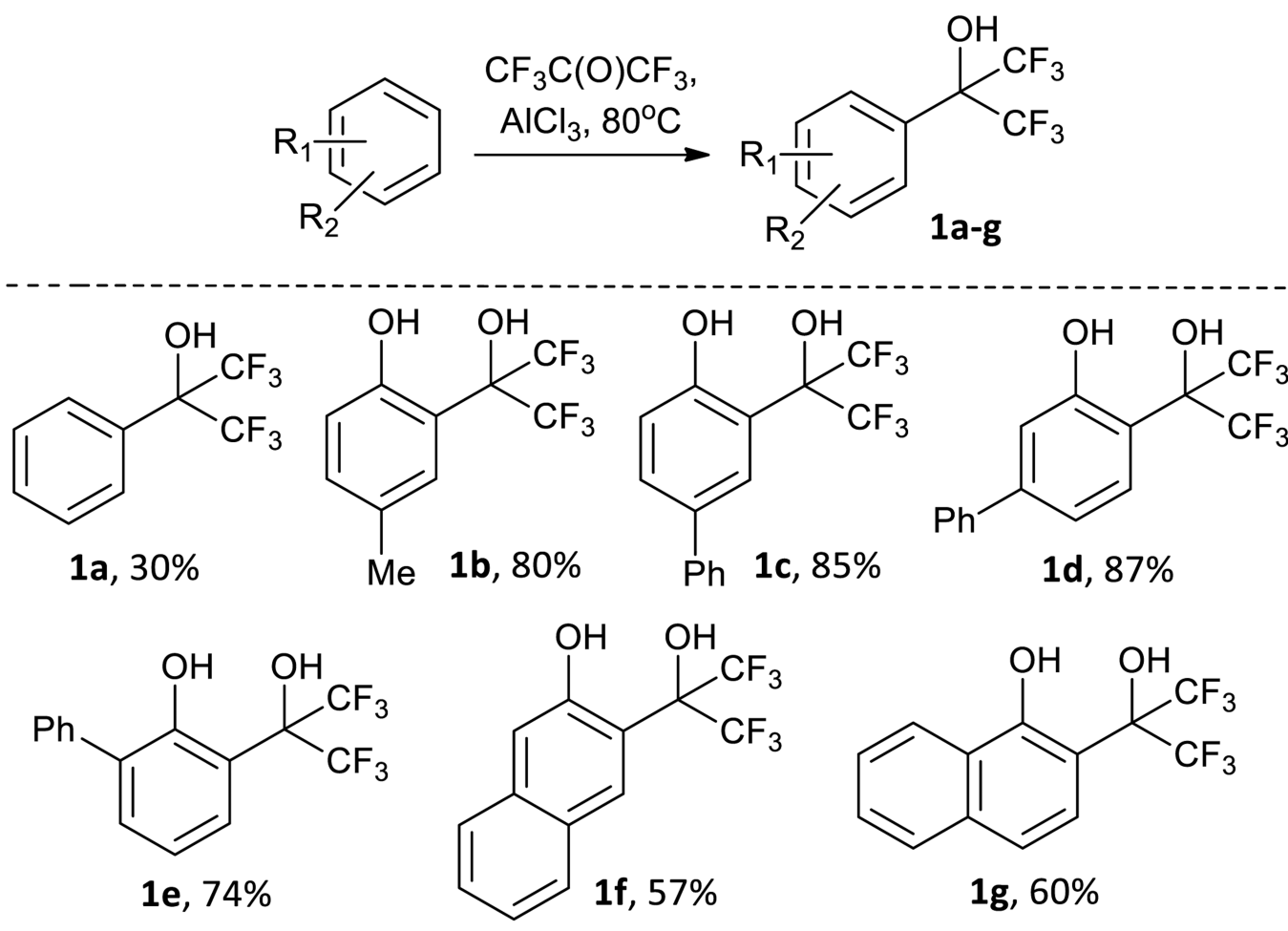


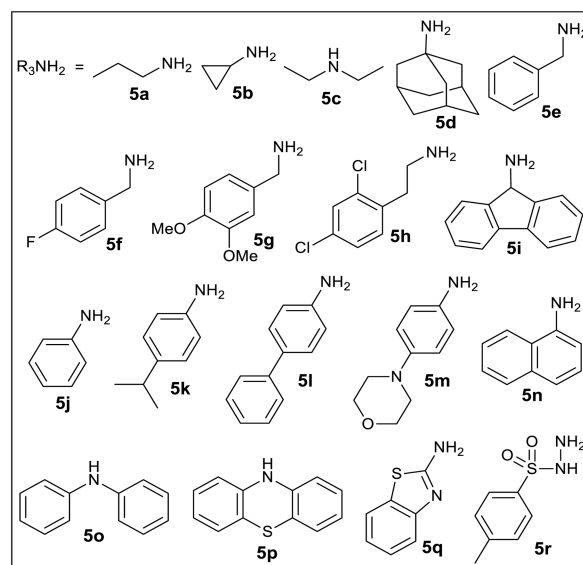
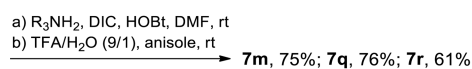
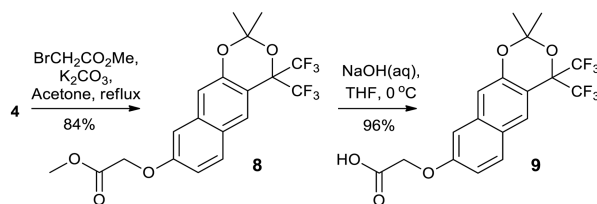
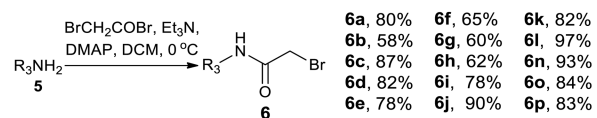
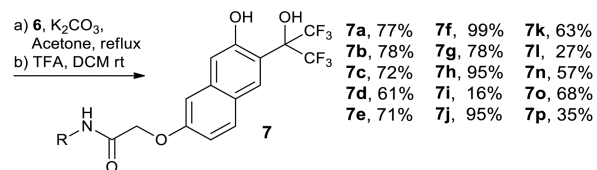
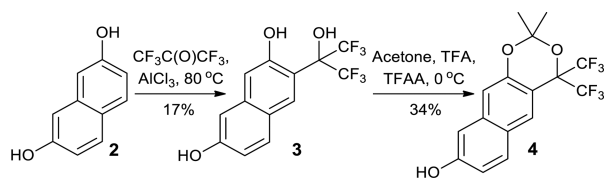
Fig. 3.
 ^{19}F NMR of selected inhibitors (upper) and ^{19}F MRI of **7p** (lower).



Scheme 1.
Design of ^{19}F MR sensitive PTP inhibitors.



Scheme 2.
Synthesis of bis(trifluoromethyl)carbinol library.



Scheme 3.
Synthesis of focused library of PTP inhibitors.

Table 1

IC₅₀ (μM) of **1a-g** for a selected panel of PTPs.

	1a	1b	1c	1d	1e	1f	1g
mPTPB	-	179.5 ± 19	351.0 ± 154	-	148.4 ± 6	105.6 ± 10	-
SHP2	-	201.8 ± 37	392.2 ± 71	-	136.0 ± 28	114.8 ± 17	-
PTP1B	-	360.2 ± 207	-	-	422.4 ± 311	260.4 ± 47	-
CD45	-	207.1 ± 17	-	-	157.2 ± 14	112.4 ± 9	-
LYP	-	302.9 ± 165	-	-	268.4 ± 149	133.9 ± 34	-
FAP-1	-	454.3 ± 754	-	-	448.8 ± 1506	127.9 ± 85	-

A “-” indicates IC₅₀ >> 500 μM.

Table 2

IC₅₀ (μM) of **7a-r** for a selected panel of PTPs.

	7a-c	7d	7e-f	7g	7h	7i	7j	7k	7l	7m	7n	7o	7p	7q	7r
mPTPB	-	-	-	18.1 ± 9.5	5.1 ± 0.4	9.4 ± 0.2	14.4 ± 1.9	7.3 ± 0.5	4.8 ± 0.1	-	4.7 ± 0.2	-	2.9 ± 0.1	2.6 ± 0.1	2.3 ± 0.1
SHP2	-	9.0 ± 2.2	-	-	6.7 ± 1.2	6.9 ± 1.4	19.0 ± 25.6	8.5 ± 1.4	3.5 ± 0.5	-	-	19.5 ± 47.8	3.2 ± 0.3	12.8 ± 3.6	20.3 ± 18.6
PTP1B	-	14.7 ± 3.0	-	-	12.6 ± 4.8	13.8 ± 2.0	-	17.2 ± 8.9	-	-	-	-	6.6 ± 1.3	-	-
CD45	-	7.6 ± 0.8	-	-	5.2 ± 0.6	6.6 ± 0.6	-	7.8 ± 0.5	3.4 ± 0.2	-	29.1 ± 38.2	14.9 ± 7.2	2.8 ± 0.2	10.9 ± 1.4	16.1 ± 5.0
LYP	-	10.1 ± 0.8	-	-	6.9 ± 1.1	7.5 ± 0.8	-	8.8 ± 1.1	-	-	-	20.6 ± 35.9	3.4 ± 0.3	14.3 ± 3.1	15.4 ± 3.1
FAP-1	-	7.4 ± 0.8	-	-	4.3 ± 1.8	5.6 ± 0.7	-	6.5 ± 0.7	2.8 ± 0.3	-	-	12.4 ± 8.3	2.2 ± 0.3	9.9 ± 1.5	14.9 ± 5.2

A “-” indicates IC₅₀ >> 20μM.